Communication

Charge Dependence of a Nanoscale Supercrystal Phase in a Supported Lipid Bilayer

Tighe A. Spurlin, and Andrew A. Gewirth

J. Am. Chem. Soc., **2007**, 129 (39), 11906-11907• DOI: 10.1021/ja074502p • Publication Date (Web): 11 September 2007

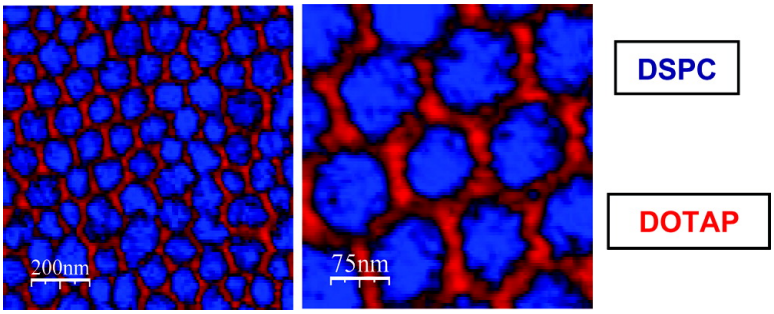

More About This Article

Additional resources and features associated with this article are available within the HTML version:

- Supporting Information
- Links to the 3 articles that cite this article, as of the time of this article download
- Access to high resolution figures
- Links to articles and content related to this article
- Copyright permission to reproduce figures and/or text from this article

View the Full Text HTML

J|A|C|S
COMMUNICATIONS

Published on Web 09/11/2007

Charge Dependence of a Nanoscale Supercrystal Phase in a Supported Lipid Bilayer

Tighe A. Spurlin and Andrew A. Gewirth*

Department of Chemistry, University of Illinois at Urbana-Champaign, 600 South Mathews, Urbana, Illinois 61801

Received June 20, 2007; E-mail: agewirth@uiuc.edu

Lipid ordered rafts (~100 nm in diameter) composed of lipids and proteins may control a range of biological functions.[1] Studies with model systems are used to determine the composition of lipids and proteins that can generate lipid rafts.[1] Ordered lipid domains of micrometer size have been seen in lipid monolayers[2] and bilayers.[3] Observations of ordered submicrometer-sized domains—possibly more relevant to biological function—are much rarer,[4] and sub-200 nm ordered domains have never been observed. Herein, we report the dependence of periodic ordered lipid domain formation near 100 nm in size on electrostatic interactions occurring within supported bilayers. The self-ordering patterns observed suggest that lipid rafts could be produced in cellular systems through charge interactions. Additionally, the structures might serve as useful templates for self-assembly applications.[5]

Ordered lipid domains have frequently been observed experimentally to form supercrystal phases with hexagonal and stripe periodicities on the micrometer scale.[6,7] Theoretical studies have linked these ordered phases in lipid systems[8,9] to similar phases first observed in type I superconductors and later seen in magnetic garnet films, block-copolymers, and ferrofluids.[9] The theoretical descriptions of supercrystal lipid phases are typically described in terms of phenomenological free energy expressed as a Ginzburg−Landau expansion.[10] Within this theoretical framework, periodic ordered lipid domains have been attributed to a competition between short-range attractive forces (van der Waals or line tension) and long-range repulsive forces (electrostatic, lipid curvature, and/or lipid stiffness).[10−12] Short-range attractive forces favor micrometer-sized domains, while repulsive forces favor sub-micrometer domains.[13,14] Utilizing AFM and mixed supported bilayers of zwitterionc distearoylphosphatidylcholine (DSPC) with cationic dioleoyltrimethylammonium propane (DOTAP) or zwitterionic dioleoylphosphatidylcholine (DOPC) we show that hexagonal supercrystal phases are dependent on the presence of long-range electrostatic repulsive forces and that the size scale of the phase depends on the zwitterionic/cationic ratio.

A series of AFM images depicting the formation of hexagonally ordered domains at different ratios of DOTAP to DSPC is shown in Figure 1A−D obtained at a temperature where DOTAP is in liquid phase, while DSPC is in gel phase. Bilayers were prepared as described previously[15] (see Supporting Information). To be certain that bilayers and not multilamellar structures formed, the thickness of DSPC/DOTAP layers were matched to previously reported values for bilayers of similar compositions (Supporting Information). Three distinct regions of bilayer can be observed for bilayers with 20 mol % DOTAP and 80 mol % DSPC. The tallest regions of the bilayer marked with a star in Figure 1A extend 1.4 ± 0.2 nm above regions marked with a diamond. Accurate determination of the depth of thin lines observed within the bilayer regions marked with a diamond was not possible because of imprecise tracing of the depth by AFM tips. Bilayers composed of

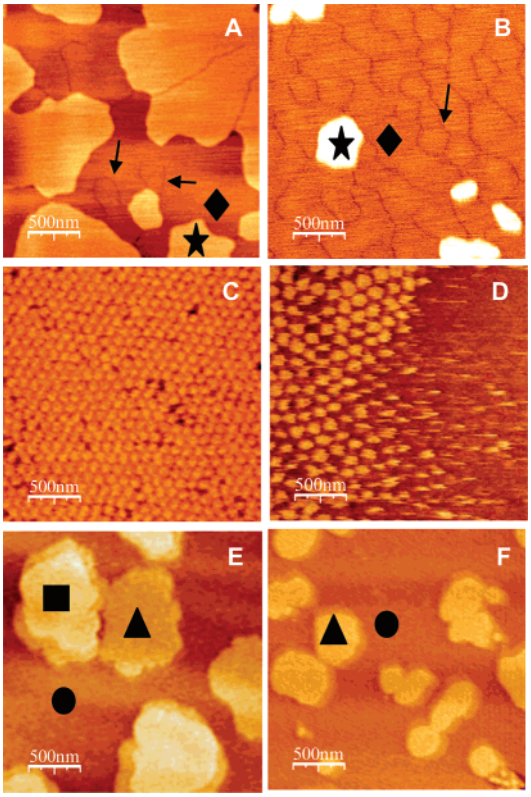

Figure 1. (A) 20 mol % DOTAP/80 mol % DSPC, (B) 30 mol % DOTAP/70 mol % DSPC, (C) 40 mol % DOTAP/60 mol % DSPC, (D) 60 mol % DOTAP/40 mol % DSPC, (E) 40 mol % DOPC/60 mol % DSPC, (F) 60 mol % DOPC/40 mol % DSPC. See main text for description of images. Images captured at 15 °C.

10 mol % DOTAP and 90 mol % DSPC did not have these features. (Supporting Information)

Increasing the DOTAP concentration resulted in increased formation of lines, as seen in Figure 1B obtained with 30 mol % DOTAP. The height between the regions of bilayer marked with the star and diamond was the same as in Figure 1A: 1.3 ± 0.2 nm. Interestingly, on isolated areas of the bilayer the thin lines form semiordered structures, as indicated by an arrow in Figure 1B. At 40 mol % DOTAP the thin lines form a network around hexagonally ordered domains as shown in Figure 1C. The hexagonal structure shown in Figure 1C was observed to be stable over 5 h at temperatures as high as 25 °C. The center−center distance between hexagonal features in this structure was determined by power spectral density analysis (Figure 2A) to be on average 100 nm.

AFM image analysis showed that bilayers composed of greater concentrations of DOTAP (Figure 1D) exhibited increased coverage by flat homogeneous fluid phase regions that closely matched the percentages of lipid vesicles (Supporting Information). This data shows that the solid support does not dramatically effect the lipid

10.1021/ja074502p CCC: $37.00

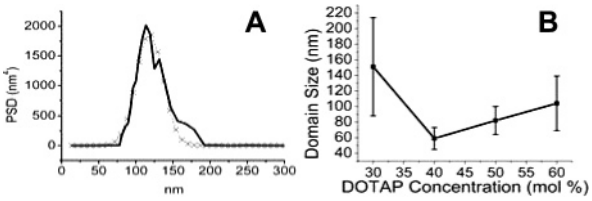

Figure 2. (A) Power spectral density analysis (solid line). A Gaussian fit of the main PSD peak resulted in a value of 118 nm (--x--). (B) Plot of domain size vs DOTAP concentration in a DSPC bilayer.

composition of the outer lipid leaflet, in which we see ordered domains.[16] The upraised lighter colored domains observed in Figure 1D were measured to extend 1.5 ± 0.2 nm above the flat homogeneous bilayer regions and network of lines that encircle the domains. The AFM images shown in Figure 1A−D strongly suggest that the fluid phase cationic DOTAP lipid is responsible for the ordered morphologies observed.

To evaluate the role of lipid charge in establishing the order seen in Figure 1B−D, measurements were obtained replacing the cationic DOTAP with the nearly identical zwitterionic DOPC lipid. As shown in Figure 1E−F, it is apparent that DOPC does not induce the same hexagonal order as DOTAP in bilayers with DSPC, over a wide composition range (Supporting Information). Instead, bilayers composed of purely zwitterionic gel and fluid phase lipids form phase separated morphologies.[15] In Figure 1E the tallest domains observed (highlighted with a square) extend 1.0 ± 0.3 nm above the regions of bilayer marked with a triangle, which are 1.0 ± 0.2 nm above the flat homogeneous regions of bilayer (emphasized with a circle). The three distinct regions of the bilayer result from symmetric leaflets of gel phase DSPC lipids (square), asymmetric DSPC−DOPC leaflets (triangle), and symmetric leaflets of liquid-phase DOPC lipids (circle).[15,17] Bilayers composed of 60 mol % DOPC and 40 mol % DSPC (Figure 1F) show similar morphologies.

The diameter of the hexagonal features was observed to be dependent on the concentration of DOTAP within the bilayer, as seen in Figure 2B. Calculations suggest that 50 nm diameter domains may be realized in bilayer systems featuring 7 D differences between charged phases.[13] This 50 nm size compares favorably with the 59 ± 14 nm diameter observed in bilayers with 40 mol % DOTAP. We now ask whether the 7 D difference is reasonable in our system. Simulations show that the inclusion of 40 mol % TAP headgroups in the bilayer increases the total potential by ∼300 mV relative to the TAP-free system. A dipole moment difference of 4.5−6 D can be approximated from this potential change (Supporting Information). Thus, it seems reasonable to suggest that increasing the DOTAP concentration in DSPC bilayers generates these ordered domains as a dipole moment difference on the order of 7 D is generated.

The upward trend in our data (Figure 2B) is likely the result of domain elongation seen in isolated portions of samples above 40 mol % (Supporting Information). Domain elongation is a well-documented feature of periodic structures that results from long-range repulsive interactions growing in relation to attractive short-range forces.[9]

In Figure 3 a schematic of the bilayer morphologies observed for supported bilayers formed from 20 mol % DOTAP/80 mol % DSPC and 40 mol % DOTAP/60 mol % DSPC is shown. The three distinct regions observed in supported bilayers of 20−30 mol % DOTAP (Figure 3A) are likely due to the formation of symmetric leaflets of gel (star) or fluid (diamond) phase lipids and asymmetric

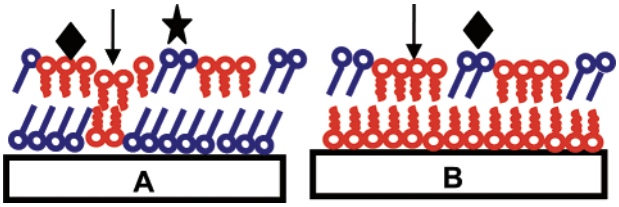

Figure 3. Schematic of hexagonal order formation: (A) 20 mol % DOTAP, (B) 40 mol % DOTAP.

leaflets of fluid lipids sitting atop gel phase lipids (arrow). Increasing the DOTAP concentration above 30 mol % results in the removal of the tallest symmetric gel domains and increases the surface area coverage of the shortest symmetrically liquid domains (Figure 3B). This schematic is supported by the following results: (1) the AFM heights measured between the bilayer regions, (2) the increase in line coverage with increasing DOTAP mol %, and (3) the observation of similar symmetric and asymmetric leaflet behaviors in bilayers of gel and fluid phase lipids.[15,17,18]

We have determined that the nanoscale hexagonal supercrystal phase observed in DSPC supported bilayers is dependent on the amount of DOTAP in the bilayer. AFM images provide evidence that the upraised hexagonally patterned domains are enriched in DSPC, while DOTAP forms an interconnected matrix. These findings indicate that 100 nm-sized lipid domains formation based on electrostatic repulsions is possible. Efforts to use the ordered bilayers as templates, through the addition of negatively charged polymers or nanoparticles to the solution above bilayers, are ongoing.

Acknowledgment. T.A.S. gratefully acknowledges support through a Hach Scientific Foundation Fellowship in chemistry. This work was supported by the National Science Foundation.

Supporting Information Available: Experimental details, bilayer cross section analysis, and the complete series of AFM images for DOPC/DSPC experiments are available in the Supporting Information. This material is available free of charge via the Internet at http://pubs.acs.org.

References

(1) Simons, K.; Ikonen, E. *Nature* **1997**, *387*, 569−572.
(2) Losche, M.; Duwe, H. P.; Moehwald, H. *J. Colloid Interface Sci.* **1988**, *126*, 432−444.
(3) Veatch, S. L.; Keller, S. L. *Biophys. J.* **2003**, *85*, 3074−3083.
(4) Rozovsky, S.; Kaizuka, Y.; Groves, J. T. *J. Am. Chem. Soc.* **2005**, *127*, 36−37.
(5) Park, C.; Yoon, J.; Thomas, E. L. *Polymer* **2003**, *44*, 6725−6760.
(6) Baumgart, T.; Hess, S. T.; Webb, W. W. *Nature* **2003**, *425*, 821−824.
(7) Moy, V. T.; Keller, D. J.; Gaub, H. E.; McConnell, H. H. *J. Phys. Chem.* **1986**, *90*, 3198−3202.
(8) Keller, D. J.; McConnell, H. M.; Moy, V. T. *J. Phys. Chem.* **1986**, *90*, 2311−2315.
(9) Seul, M.; Andelman, D. *Science* **1995**, *267*, 476−483.
(10) Andelman, D.; Brochard, F.; Joanny, J. F. *J. Chem. Phys.* **1987**, *86*, 3673−3681.
(11) Liu, J.; Qi, S.; Groves, J. T.; Chakraborty, A. K. *J. Phys. Chem. B* **2005**, *109*, 19960−19969.
(12) McConnell, H. M.; De Koker, R. *Langmuir* **1996**, *12*, 4897−4904.
(13) Liu, J.; Groves, J. T.; Chakraborty, A. K. *J. Phys. Chem. B* **2006**, *110*, 8416−8421.
(14) Travesset, A. *J. Chem. Phys.* **2006**, *125*, 084905/1−084905/12.
(15) Lin, W.-C.; Blanchette, C. D.; Ratto, T. V.; Longo, M. L. *Biophys. J.* **2006**, *90*, 228−237.
(16) Junglas, M.; Danner, B.; Bayerl, T. M. *Langmuir* **2003**, *19*, 1914−1917.
(17) Lin, W.-C.; Blanchette, C. D.; Longo, M. L. *Biophys. J.* **2007**, *92*, 2831−2841.
(18) Rinia, H. A.; Kik, R. A.; Demel, R. A.; Snel, M. M. E.; Killian, J. A.; van der Eerden, J. P. J. M.; de Kruijff, B. *Biochemistry* **2000**, *39*, 5852−5858.

JA074502P